ELSEVIER

Journal of Nuclear Materials 275 (1999) 186–193

journal of nuclear materials

www.elsevier.nl/locate/jnucmat

Electrolytic hydrogenation and its isotope effect in Zr and Pd studied by ERDA and SIMS techniques

Yasuhisa Oya [a,*], Tatsuya Suzuki [b], Koichi Iinuma [a], Kenji Morita [c], Tomoaki Horikawa [c], Katsunori Abe [a], Makoto Okamoto [a,1]

[a] *Department of Quantum Science and Energy Engineering, Graduate School of Engineering, Tohoku University, Aramaki, Aoba-ku, Sendai 980-8579, Japan*

[b] *The Wakasa Wan Energy Research Center, 64-52-1, Nagatani, Tsuruga 914-0192, Japan*

[c] *Department of Crystalline Materials Science, Graduate School of Engineering, Nagoya University, Furo-cho, Chikusa-ku, Nagoya 464-8603, Japan*

Received 22 September 1998; accepted 5 April 1999

Abstract

In order to study the isotope effect in hydrogen absorption of Zr and Pd metals, protium and deuterium were charged electrolytically and their depth profiles were measured by elastic recoil detection analysis (ERDA) and secondary ion mass spectrometry (SIMS) techniques. The loading ratios of hydrogen isotopes were compared. The loading ratios of H(D)/M are calculated from the ERDA and RBS spectra. In the separate electrolysis, the isotope ratios (D/H) in Zr and Pd were 2/3 and 1, respectively. However, the isotope ratio in Zr was 1/3 in the simultaneous electrolysis, but that in Pd was 1/10. The results of the SIMS measurements were consistent with those of the ERDA measurements. An electrolysis model was proposed to explain the experimental results. Based on the model, it is found that the difference between the fluxes of hydrogen ions gives rise to the isotope effect in Pd. In Zr, however, the conversion frequency and the recombination rate constant dominate the isotope effect.

PACS: 82.20.T; 31.30.G; 68.35.J

1. Introduction

The hydrogen storage metals are important to develop energy systems without CO_2 release [1]. The required function of the metals in the energy systems is not only to store and carry the hydrogen but also to separate the hydrogen isotopes and to store the tritium, especially for the future nuclear fusion reactor. These functions can be limited by various factors describing the behavior of hydrogen in metals and their isotope effect. However, basic mechanism of hydrogenation and its isotope effects have not been clarified yet sufficiently.

So far, to study the isotope effect of hydrogen absorption by electrolysis, the two pure metals, Zr and Pd, have been picked up from hexagonal closest packed (hcp) structure and face-centered cubic (fcc) structure, respectively. There are two tetrahedral (T) sites and one octahedral (O) site per unit lattice in both structures. The hydrogen atoms in PdH_x occupy O-site rather than T-site as hydrogen is charged electrolytically, while the hydrogen atoms in ZrH_x tend to locate at T-site at first [2]. This occupation rule has been connected to large hydrogen isotope effects. However, the kinetics of hydrogenation have not been taken into account for the explanation. In order to clarify the kinetics, it is important to study the absorption and distribution of hydrogen isotopes (H and D) in both metals by simultaneous electrolysis of $H_2O + D_2O$.

In this paper, the separate electrolysis and the simultaneous electrolysis with water whose isotope ratio

* Corresponding author. Tel.: +81-22 217 7936; fax: +81-22 217 7900; e-mail: yoya@vesper.qse.tohoku.ac.jp

[1] Professor Makoto Okamoto passed away on 4 May 1998.

0022-3115/99/$ - see front matter
PII: S0022-3115(99)00115-4

between protium and deuterium is 1 : 1 are performed for one day to absorb the hydrogen isotopes. After performing the electrolysis, the loading hydrogen isotope ratio is measured by means of the elastic recoil detection analysis (ERDA) and the secondary ion mass spectrometry (SIMS) techniques. The difference between the isotope ratios in Pd and Zr is quantitatively explained in terms of the solution of a set of the mass balance equations which have been developed according to an electrolysis model proposed for hydrogen isotopes absorption.

2. An electrolysis model for the hydrogen isotopes absorption

A hydrogen isotopes absorption process connected to the present electrolysis is modeled in Fig. 1. All the ions adsorbed on the surface are assumed to be converted to the atoms, all of which are absorbed into the metal or recombined into molecules on the metal surface. As can be seen from Fig. 1, the processes involved are divided into three parts: adsorption, absorption and recombination.

In the separate electrolysis, the time evolutions of the concentrations of protium, n_{ad}^{H}, and deuterium, n_{ad}^{D}, adsorbed at the surface are described respectively by Eqs. (1) and (2),

$$\frac{dn_{ad}^{H}}{dt} = \phi_{H^+} n_e \sigma_{ad}^{H} - \xi_{ab}^{H} n_{ad}^{H} - 2K^{HH}\left(n_{ad}^{H}\right)^2, \tag{1}$$

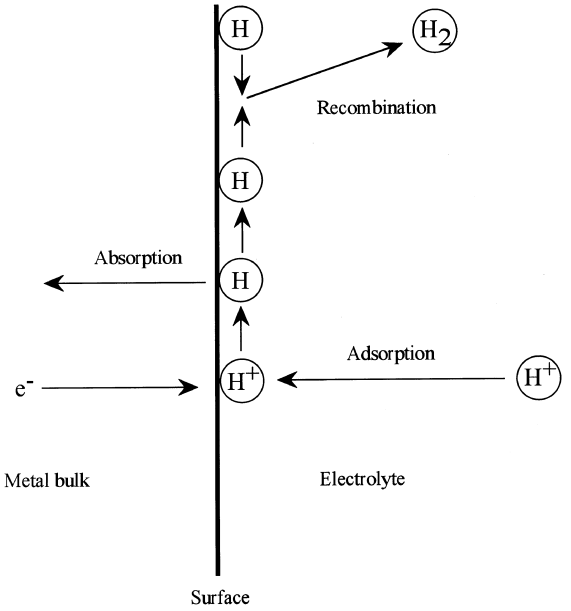

Fig. 1. An electrolysis model for the hydrogen isotopes absorption processes in metal.

$$\frac{dn_{ad}^{D}}{dt} = \phi_{D^+} n_e \sigma_{ad}^{D} - \xi_{ab}^{D} n_{ad}^{D} - 2K^{DD}\left(n_{ad}^{D}\right)^2, \tag{2}$$

where ϕ_{H^+} and ϕ_{D^+} are the fluxes of proton and deuteron to the cathode surface from electrolyte, respectively. $\sigma_{ad}^{H}, \sigma_{ad}^{D}$, ξ_{ab}^{H} and ξ_{ab}^{D} are the adsorption cross-sections and absorption conversion frequency of H and D, respectively. The K^{HH} and K^{DD} represent the rate constants of H–H and D–D recombination. The n_e is the neutralization probabilities of H^+ and D^+ on the cathode surface. In these equations, the first, second and third terms correspond to the adsorption, the absorption and the recombination, respectively. The rates of the concentration change of the absorbed protium and deuterium are expressed as follows:

$$\frac{dn_{ab}^{H}}{dt} = \xi_{ab}^{H} n_{ad}^{H}, \qquad \frac{dn_{ab}^{D}}{dt} = \xi_{ab}^{D} n_{ad}^{D}. \tag{3}$$

In the present study, it is assumed that the absorbed hydrogen atoms form the hydride and the hydride does not dissolve as long as the specimen is not heated and that hydrogen diffusion in the hydride is so fast. Therefore, Eq. (3) represents the growth of hydride layers, namely the increase in thickness of the hydride layers. In such a case, the amounts of adsorbed protium and deuterium reach a quasi-equilibrium, namely, $dn_{ad}^{H}/dt = 0$ and $dn_{ad}^{D}/dt = 0$, just after start of the electrolysis, thus the values of n_{ad}^{H} and n_{ad}^{D} are expressed, using the Taylor expansion, from Eqs. (1) and (2) into Eqs. (4) and (5) on the assumption that $(\xi_{ab})^2$ is larger than $8K\phi$ (absorption-controlled).

$$n_{ad}^{H} = \frac{-\xi_{ab}^{H} + \sqrt{\left(\xi_{ab}^{H}\right)^2 + 8K^{HH}\phi_{H^+}}}{4K^{HH}} \cong \frac{\phi_{H^+}}{\xi_{ab}^{H}}\left(1 - \frac{4K^{HH}\phi_{H^+}}{\left(\xi_{ab}^{H}\right)^2}\right), \tag{4}$$

$$n_{ad}^{D} = \frac{-\xi_{ab}^{D} + \sqrt{\left(\xi_{ab}^{D}\right)^2 + 8K^{DD}\phi_{D^+}}}{4K^{DD}} \cong \frac{\phi_{D^+}}{\xi_{ab}^{D}}\left(1 - \frac{4K^{DD}\phi_{D^+}}{\left(\xi_{ab}^{D}\right)^2}\right). \tag{5}$$

In derivation of these equations, it was assumed for simplicity that $n_e\sigma_{ad}^{H}$ and $n_e\sigma_{ad}^{D}$ are unity. In the model, the adsorption process is followed by the recombination process and this means that K^{HH} depends on $1/\phi_{H^+}^2$. When the flux of H^+ and D^+ ions is very high, which means that the second terms in the larger parenthesis of Eqs. (4) and (5) are negligible small compared with unity, the values of n_{ad}^{H} and n_{ad}^{D} are absorption-controlled and described by ϕ_{H^+}/ξ_{ab}^{H} and ϕ_{D^+}/ξ_{ab}^{D}, respectively. In the recombination-controlled case, the terms of ξ_{ab}^{H} and ξ_{ab}^{D} are assumed to be negligibly small in Eqs. (1) and (2). In this case, the values of n_{ad}^{H} and n_{ad}^{D} are given by $\sqrt{\phi_{H^+}/2K^{HH}}$ and $\sqrt{\phi_{D^+}/2K^{DD}}$, respectively. These

equations give the isotope ratio of hydrogen loading when the current in electrolysis of H_2O is equal to that in electrolysis of D_2O.

In the case of the simultaneous electrolysis, the mass balance equations are expressed by Eqs. (6) and (7),

$$\frac{dn_{ad}^{H}}{dt} = \phi_{H^+} n_e \sigma_{ad}^{H} - \xi_{ab}^{H} n_{ad}^{H} - 2K^{HH}\left(n_{ad}^{H}\right)^2 - K^{HD} n_{ad}^{H} n_{ad}^{D}, \tag{6}$$

$$\frac{dn_{ad}^{D}}{dt} = \phi_{D^+} n_e \sigma_{ad}^{D} - \xi_{ab}^{D} n_{ad}^{D} - 2K^{DD}\left(n_{ad}^{D}\right)^2 - K^{HD} n_{ad}^{H} n_{ad}^{D}, \tag{7}$$

where K^{HD} represents the rate constant of H–D recombination. Eqs. (6) and (7) can not be easily solved, because the product terms of n_{ad}^{H} and n_{ad}^{D} are included. However, the approximate solutions can be obtained both in the absorption-controlled and recombination-controlled cases. The solutions in the former case are the same as those in the separate electrolysis.

In the recombination-controlled case, the concentrations of adsorbed protium and deuterium at the quasi-equilibrium are expressed by the following equations:

$$\left(n_{ad}^{H}\right)^2 = \frac{8\phi_{H^+} + (\phi_{D^+} - \phi_{H^+})A}{4K^{HH}(4-A)} + \frac{\sqrt{\{8\phi_{H^+} + (\phi_{D^+} - \phi_{H^+})A\}^2 - 16\phi_{H^+}^2(4-A)}}{4K^{HH}(4-A)}, \tag{8}$$

$$\left(n_{ad}^{D}\right)^2 = \frac{8\phi_{D^+} + (\phi_{H^+} - \phi_{D^+})A}{4K^{DD}(4-A)} + \frac{\sqrt{\{8\phi_{D^+} + (\phi_{H^+} - \phi_{D^+})A\}^2 - 16\phi_{D^+}^2(4-A)}}{4K^{DD}(4-A)}, \tag{9}$$

where $A = K^{HD^2}/K^{HH}K^{DD}$. The solutions of the mass balance equations, n_{ad}^{H} and n_{ad}^{D}, give the isotope ratio of loading hydrogen atoms induced by simultaneous electrolysis of $H_2O + D_2O$.

3. Experimental

3.1. Specimen

The Zr and Pd metal specimens used were supplied by Nilaco and Tanaka Kikinzoku, respectively. The purity of Zr was 99.7% and that of Pd was 99.99%. Typical impurities in Zr and Pd were Hf and Ca, respectively. The size of the metal specimens was $10 \times 25 \times 1.0$ mm each. The pretreated procedure was as follows: The surface of metals were polished mechanically by SiC carbimet paper of #240 $\sim$ #800, diamond suspensions of three and one micron size, and colloidal Si liquid. The layers of 0.1 mm in thickness were lost at each sides by the polishing. After the polishing, Zr samples were annealed at 973 K and Pd samples were annealed at 1123 K for 10 h in vacuum of 10^{-7} Torr.

3.2. Electrolysis

The light water specimen used was ion exchanged water and the heavy water used was purchased from Isotec. Both the light water and the heavy water were distilled with potassium permanganate as a strong oxidation reagent. Three kinds of electrolyte, 1.0 M LiOD, LiOH and LiOD + LiOH electrolyte, were prepared by dissolving the metallic lithium that was packed under argon gas and purchased from Soekawa Chemicals, in the distilled water. In the LiOD + LiOH mixture electrolyte, the mole ratio of D and H was 1 : 1.

The detail of the electrolysis cell is shown schematically in Fig. 2. The electrolysis cell was made of Pyrex glass. The Pd cathode was positioned in the center of the electrolysis cell. The Pt anode wire was placed around the Pd cathode like spiral. The five resistance thermometers made of SUS316 were used to measure the electrolyte and cooling water; three were installed in the electrolyte and the two were located in the inlet and outlet of the cooling water, respectively. The temperature of the electrolyte was limited to be 297 K throughout the operation. The amount of the electrolyte was kept to be 400 ml by the electrolyte level system. The

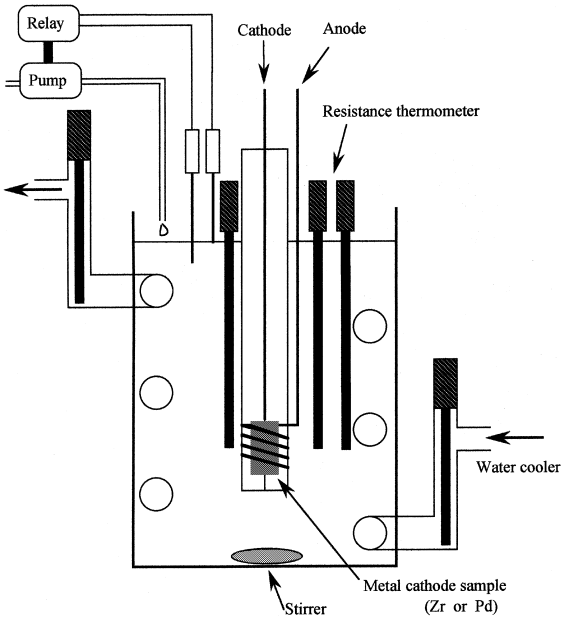

Fig. 2. The schematic drawing of the electrolysis cell.

current density was 800 mA/cm^2. The ambient temperature was also limited at 297 ± 1 K. The electrolysis was performed for one day in order to guarantee the achievement of the equilibrium hydride formation over the whole specimen, although we measured change of the hydrogen loading ratio in Pd by use of resistance measurement and found that the loading ratio was saturated less than 30 min. After the saturation which means the achievement of the equilibrium hydride formation over the whole specimen, protium and deuterium are expected to be charged in excess of the equilibrium hydride composition. Therefore, the specimens were placed in electrolyte for 2 days after stop of the electrolysis, thus the excess hydrogen atoms being expected to desorb outside of the specimen. Also, the excess hydrogen atoms would be desorbed when the specimen were placed in the vacuum chamber of ERDA and SIMS instruments. We believe that the ERDA measurement gives the hydride composition, namely saturated loading ratio which is not changed as long as the specimen is heated.

3.3. ERDA measurements

The 2.5 MeV Van de Graaff accelerator at Nagoya University was used to generate the 1.7 MeV He^+ ion beams [3,4]. The geometry used in our ERDA measurements is illustrated in Fig. 3. The primary beam of 1.7 MeV He^+ ions was directed onto the sample at an angle of 80° to the surface normal. The typical ion beam size was 1mm in diameter. The recoiled hydrogen isotopes were detected in a Si surface barrier detector (SSD) at a forward angle of 80° to the surface normal, which is so called ERD. The Mylar thin film was used in front of the SSD detector to get rid of the scattered helium ions and other heavy ions. The He^+ ions scattered at the angle of 50° to the surface normal were also detected, which is so called RBS. The fluence of He^+ ions bombarded on the specimen during the ERDA measurement is monitored simultaneously by means of the RBS measurements.

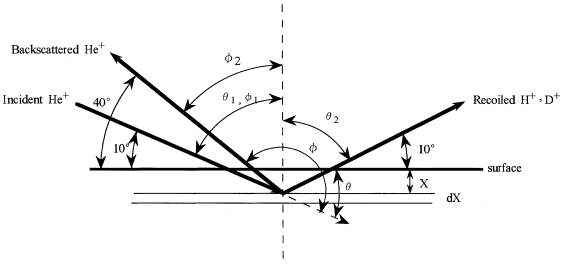

Fig. 3. The geometrical arrangement of the incident beam, scattered He^+ and recoiled H^+ and D^+ to the surface normal of the sample.

The loading ratios for both hydrogen isotopes were obtained as follows. The amount of the recoiled hydrogen particles, $H_{\mathrm{H\ in\ Me}}$ can be represented by Eq. (10),

$$H_{\mathrm{H\ in\ Me}} = Q_{\mathrm{He}}^{\mathrm{Me}}\Omega_\theta\sigma_{\mathrm{recoil}}^{\mathrm{He}\to\mathrm{H}}(E_0)N_{\mathrm{H}}\,\mathrm{d}x = Q_{\mathrm{He}}^{\mathrm{Me}}\Omega_\theta\sigma_{\mathrm{recoil}}^{\mathrm{He}\to\mathrm{H}}(E_0)\frac{\mathrm{d}E}{[\varepsilon]_{\mathrm{ERD}}^{\mathrm{Me}}}\frac{N_{\mathrm{H\ in\ Me}}}{N_{\mathrm{Me}}}, \tag{10}$$

where Me is Zr or Pd, $Q_{\mathrm{He}}^{\mathrm{Me}}$ is the number of incident He^+ ions, Ω_θ is the solid angle subtended by the SSD detector, $\sigma_{\mathrm{recoil}}^{\mathrm{He}\to\mathrm{H}}(E_0)$ is the Rutherford recoil cross-section for hydrogen, E_0 is the incident energy of He^+ and $[\varepsilon]_{\mathrm{ERD}}^{\mathrm{Me}}$ is the average stopping cross-section of target atom for recoiled hydrogen ions, respectively. The x is the depth of H atoms retained and N_{H} is the density of H retained. The amount of the backscattered He^+ ions is also given by Eq. (11),

$$H_{\mathrm{He}}^{\mathrm{Me}} = Q_{\mathrm{He}}^{\mathrm{Me}}\Omega_\phi\sigma_{\mathrm{scattering}}^{\mathrm{He}\to\mathrm{Me}}(E_0)N_{\mathrm{Me}}\,\mathrm{d}x = Q_{\mathrm{He}}^{\mathrm{Me}}\Omega_\phi\sigma_{\mathrm{scattering}}^{\mathrm{He}\to\mathrm{Me}}(E_0)\frac{\mathrm{d}E}{[\varepsilon]_{\mathrm{RBS}}^{\mathrm{Me}}}, \tag{11}$$

where $Q_{\mathrm{scattering}}^{\mathrm{He}\to\mathrm{Me}}$ is the Rutherford backscattering cross-section of He^+ ions. The $[\varepsilon]_{\mathrm{RBS}}^{\mathrm{Me}}$ is the average stopping cross-section of target atoms for backscattered He^+ ions. For estimation of the hydrogen amounts, the values of Ω_θ and Ω_ϕ are required. In order to get rid of the uncertainty [5,6], the values of Ω_θ and Ω_ϕ obtained with graphite were used in the present experiment. Therefore, the protium loading ratio and the deuterium loading ratio are expressed by Eqs. (12) and (13), respectively.

$$\frac{N_{\mathrm{H\ in\ Me}}}{N_{\mathrm{Me}}} = \frac{H_{\mathrm{H\ in\ Me}}}{H_{\mathrm{H\ in\ C}}}\frac{H_{\mathrm{He}}^{\mathrm{C}}}{H_{\mathrm{He}}^{\mathrm{Me}}}\frac{\sigma_{\mathrm{scattering}}^{\mathrm{He}\to\mathrm{Me}}(E_0)}{\sigma_{\mathrm{scattering}}^{\mathrm{He}\to\mathrm{C}}(E_0)}\frac{[\varepsilon]_{\mathrm{RBS}}^{\mathrm{C}}}{[\varepsilon]_{\mathrm{RBS}}^{\mathrm{Me}}}\frac{[\varepsilon]_{\mathrm{ERD}}^{\mathrm{Me}}}{[\varepsilon]_{\mathrm{ERD}}^{\mathrm{C}}} \times \frac{N_{\mathrm{H\ in\ C}}}{N_{\mathrm{C}}}, \tag{12}$$

$$\frac{N_{\mathrm{D\ in\ Me}}}{N_{\mathrm{Me}}} = \frac{H_{\mathrm{D\ in\ Me}}}{H_{\mathrm{H\ in\ C}}}\frac{H_{\mathrm{He}}^{\mathrm{C}}}{H_{\mathrm{He}}^{\mathrm{Me}}}\frac{\sigma_{\mathrm{scattering}}^{\mathrm{He}\to\mathrm{Me}}(E_0)}{\sigma_{\mathrm{scattering}}^{\mathrm{He}\to\mathrm{C}}(E_0)}\frac{[\varepsilon]_{\mathrm{RBS}}^{\mathrm{C}}}{[\varepsilon]_{\mathrm{RBS}}^{\mathrm{Me}}}\frac{[\varepsilon]_{\mathrm{ERD}}^{\mathrm{Me}}}{[\varepsilon]_{\mathrm{ERD}}^{\mathrm{C}}} \times \frac{N_{\mathrm{H\ in\ C}}}{N_{\mathrm{C}}}\frac{\sigma_{\mathrm{recoil}}^{\mathrm{He}\to\mathrm{H}}(E_0)}{\sigma_{\mathrm{recoil}}^{\mathrm{He}\to\mathrm{D}}(E_0)}, \tag{13}$$

The average stopping cross-sections for recoiled hydrogen ions and for backscattered He^+ ions are represented by Eqs. (14) and (15), respectively.

$$[\varepsilon]_{\mathrm{ERD}}^{\mathrm{Me}} = k_2\frac{\varepsilon^{\mathrm{He}\to\mathrm{Me}}(E_0)}{\cos\theta_1} + \frac{\varepsilon^{\mathrm{H}\to\mathrm{Me}}(k_2E_0)}{\cos\theta_2}. \tag{14}$$

$$[\varepsilon]_{\mathrm{RBS}}^{\mathrm{Me}} = k_1\frac{\varepsilon^{\mathrm{He}\to\mathrm{Me}}(E_0)}{\cos\phi_1} + \frac{\varepsilon^{\mathrm{H}\to\mathrm{Me}}(k_1E_0)}{\cos\phi_2}. \tag{15}$$

The typical values for calculating the average stopping power of $[\varepsilon]_{\mathrm{ERD}}^{\mathrm{Me}}$ and $[\varepsilon]_{\mathrm{RBS}}^{\mathrm{Me}}$ are obtained from Refs. [7,8],

Table 1
Typical value of the average stopping cross section and scattering cross section

	$[\varepsilon]_{H,ERD}$ (10^{-15} eV cm^2/atom)	$[\varepsilon]_{D,ERD}$ (10^{-15} eV cm^2/atom)	$[\varepsilon]_{RBS}$ (10^{-15} eV cm^2/atom)	$[\varepsilon]_{scattering}$ (E_0 cm^2/atom)
Zr	434.22	584.26	691.26	3.286×10^{-24}
Pd	415.13	557.50	643.35	4.350×10^{-24}
C	123.33		105.17	6.036×10^{-26}

Table 2
The RBS and ERDA experimental data of graphite used for calculating the loading ratio of hydrogen isotope in metal

$H_{H\ in\ C}$ (counts)	H^C_{He} (counts)	$N_{H\ in\ C}/N_C$
555	99	0.4

which are listed in Table 1. In the values of $[\varepsilon]^{Me}_{ERD}$ and $[\varepsilon]^{Me}_{RBS}$, the stopping cross-section of hydrogen atoms charged were not taken into account. The stopping power of hydrogen atom for 1.7 MeV He^+ ions is 8.72×10^{-15} eV cm^2/atom. This value correspond to about 7% of the stopping powers of Zr and Pd for He^+ ions. The loading ratio given by Eqs. (12) and (13) are proportional to the ratio of $[\varepsilon]^{Me}_{ERD}/[\varepsilon]^{Me}_{RBS}$, thus the contribution of the hydrogen stopping cross-sections become much smaller than the value. The Rutherford scattering cross-section was used for the scattering cross-sections of He^+ ions scattered by metal or graphite. But, the recoil cross-sections for hydrogen and deuterium were assumed to be the cross-sections at 1.9 MeV [3,9]. The RBS and ERDA experimental data of graphite used for calculating the loading ratio of hydrogen isotopes in metal are summarized in Table 2.

3.4. SIMS measurements

The SIMS (Model IMF-4f, CAMECA/France) was carried out at Tokyo Institute of Technology, using the primary ion (O_2^+) of 15.1 keV accelerated energy and a beam current of 4×10^{-7} A at 30° from the surface normal. Before measuring the depth profile of the elements, the resolution between H_2^+ and D^+ was checked, which is shown in Fig. 4. The counts of 2.014 amu correspond to D^+, exactly. The depth scale for the SIMS profiles was determined from the relation between the sputtering time and the stylus roughness measurement by the Dektak profilometer [10,11]. Typical sputtering rates were about 0.015 μm/s.

4. Results

4.1. The estimation of the loading ratio of protium and deuterium

Typical RBS and ERDA spectra are shown for the specimens, Pd (○) and Zr (×) loaded by simultaneous electrolysis of LiOH + LiOD in Figs. 5 and 6, respectively. In Fig. 5, the energies (Channel numbers) of He^+ ions backscattered from Pd and Zr specimens, and Fe and Pt impurities are shown by the arrows with the elemental symbols, respectively. It is seen from Fig. 5 that the Pt peak in 875 channel of the RBS spectra correspond to platinum, which is used as anode. It is also seen from Fig. 5 that Fe peak corresponds to iron, which is a main component of SUS and is used as resistance thermometers. These facts indicate that the small amounts of these impurities are deposited on the cathode surface

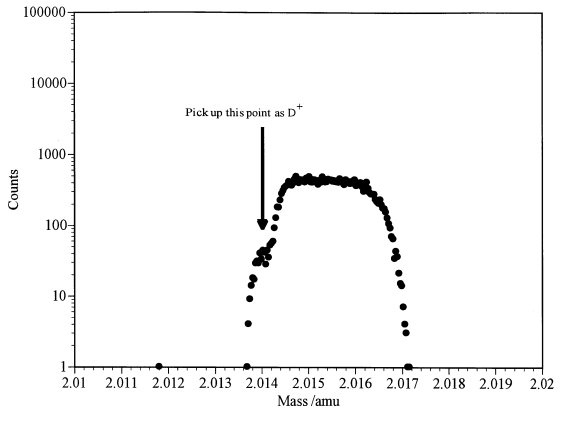

Fig. 4. The resolution of H_2^+ and D^+ in SIMS.

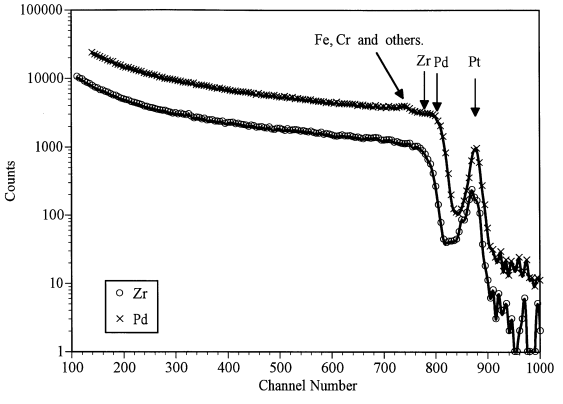

Fig. 5. The RBS spectra of 1.7 MeV He^+ ion beam from Zr (○) and Pd (×) samples loaded LiOD + LiOH mixture electrolyte.

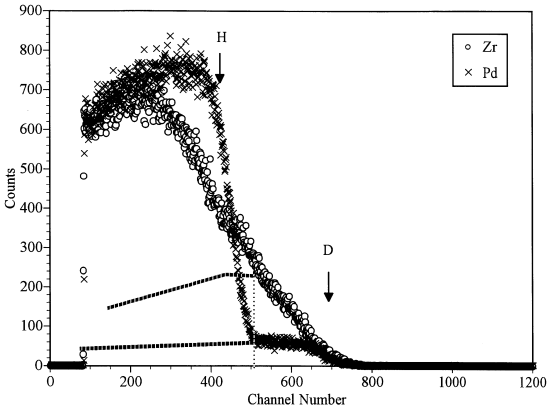

Fig. 6. The ERDA spectra of D^+ and H^+ recoiled from Zr (○) and Pd (×) samples loaded with LiOD + LiOH mixture electrolyte.

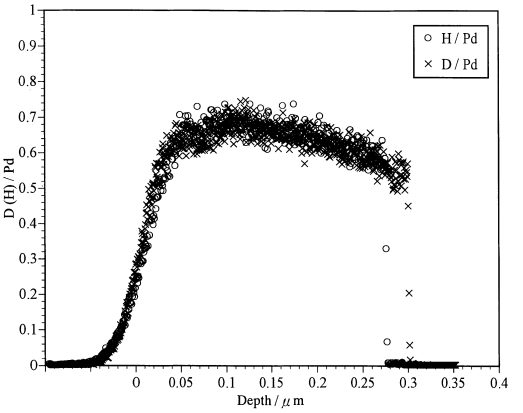

Fig. 8. The depth profiles of the D (○) or H (×) loaded in Pd with LiOD or LiOH electrolyte.

during the electrolysis. But, the small amounts of these impurities are not considered to influence the adsorption and absorption of the hydrogen isotopes, essentially. In Fig. 6, the energies of D^+ and H^+ ions recoiled at the target surface also are shown by the arrows with the symbols D and H, respectively.

The depth profiles of protium and deuterium in Zr and Pd loaded with the LiOD or LiOH electrolyte are shown in Figs. 7 and 8, respectively. Fig. 7 depicts that the amount of protium loaded in Zr is saturated to 2.5 as the depth increases and that of deuterium loaded is 1.7. It is seen from Fig. 7 that the loading ratio of H/Zr is about 1.5 times as large as that of D/Zr. On the other hand, in Pd the concentration of D/Pd, 0.7, is nearly equal to that of H/Pd.

The depth profiles of protium and deuterium loaded in Zr and Pd with LiOD + LiOH mixture electrolyte are illustrated in Figs. 9 and 10, respectively. As seen from Fig. 6, the ERD spectrum of D retained is overlapped over that of H retained. The distributions of absolute number densities of H and D are determined from the ERD spectra. In conversion of ERD spectra to the depth profiles of H and D, the overlapping tails of the ERD spectrum of D were assumed to be dotted lines based on the SIMS depth profiles shown in Fig. 11. It is seen from Fig. 9 that the amount of H is 1.2 and that of D loaded reaches to almost 0.4 in Zr. On the other hand, the amount of H loaded in Pd is 0.7 and that of D is only 0.07. This indicates that there is great isotope effect in the amounts of H and D loaded in metal cathode by simultaneous electrolysis.

The D/H ratios are calculated from these figures to be D/H≒1/3 in Zr and D/H≒1/10 in Pd. These results indicate that the absorption isotope ratios in cathode depend strongly on the material.

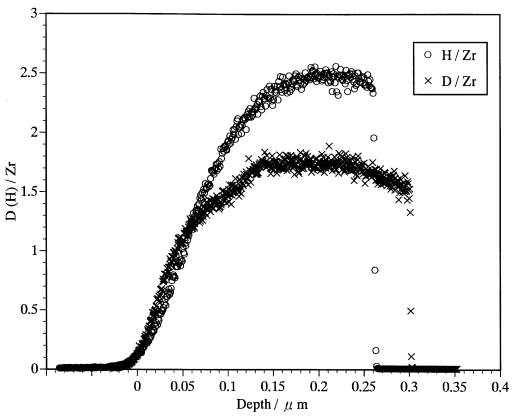

Fig. 7. The depth profiles of the D (○) or H (×) loaded in Zr with LiOD or LiOH electrolyte.

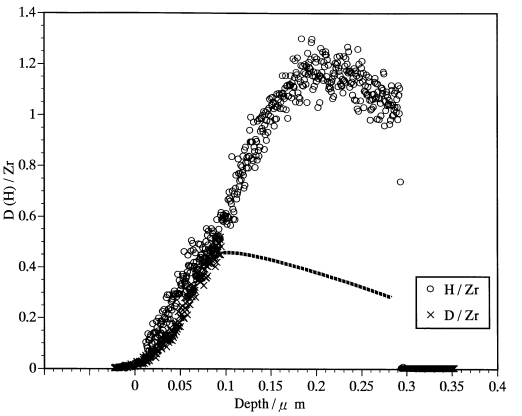

Fig. 9. The depth profiles of the D (○) and H (×) loaded in Zr with LiOD + LiOH mixture electrolyte.

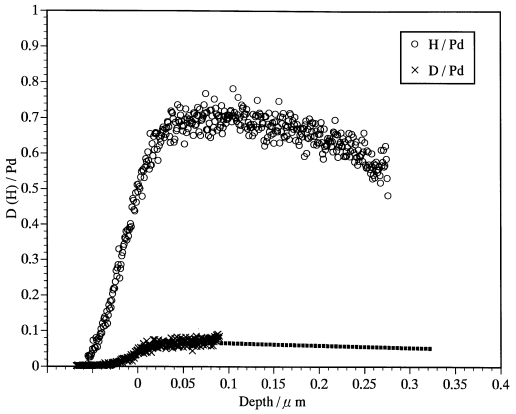

Fig. 10. The depth profiles of the D (○) and H (×) loaded in Pd with LiOD + LiOH mixture electrolyte.

4.2. The depth profiles of the hydrogen isotopes by SIMS

In order to obtain the distribution of the hydrogen isotopes loaded in deep layer of Pd and Zr, SIMS analysis is carried out. Fig. 11 shows the depth profiles of H^+ and D^+ in Zr and Pd, respectively. The depth profiles indicate that H^+ and D^+ are uniformly absorbed in Zr except in the surface region. It is also seen that the hydrogen concentrations are reduced in the surface layers of Zr, clearly. This trend coincides with the ERDA measurement. This result might be ascribed to formation of oxide layers at the surface of Zr cathode. On the other hand, the depth profiles of H^+ and D^+ in Pd are absolutely different from those in Zr. The difference between the secondary ion counts of H^+ and D^+ is reduced as the depth increase beyond about 1.5 μm. This means that D/H ratio in the surface layers is different from that in the metal bulk of Pd. To clarify this reason, the additional experiments should be carried out in detail by changing the parameters of current density and electrolysis period.

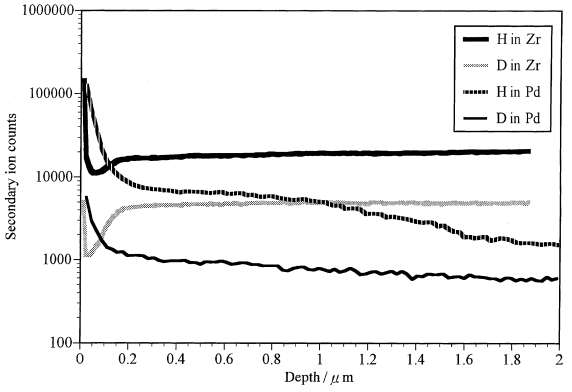

Fig. 11. The depth profiles of H^+ and D^+ ions by use of O_2^+ ions as primary ions in SIMS.

The intensity ratios of H^+ and D^+ in Zr and Pd at the depth of 0.2–0.4 μm are about 1/3 and 1/10, respectively and these results are good agreement with the results of ERDA measurement.

5. Discussion

As has been described in the model, the absorption process is divided into the three reactions. To clarify the dominant reaction, we examine the results of the separate electrolysis with Pd and Zr and the simultaneous electrolysis with Pd and Zr.

5.1. Electrolysis with Pd

In the second section, the two controlled cases, the absorption-controlled and the recombination-controlled cases have been introduced. In the preceding section, it has been shown that the ratio of H and D under the equilibrium condition is almost unity. Since the value of ϕ_{D^+}/ϕ_{H^+} in the present study is unity under the same current density condition., the isotope ratio for Pd in this case is regarded to indicate that the second term in the parenthesis of Eqs. (4) and (5) should be negligibly small compared with unity rather than that $\xi_{ab}^{H}/\sqrt{K^{HH}} = \xi_{ab}^{D}/\sqrt{K^{DD}}$, namely the loading process is absorption-controlled. On the other hand, the isotope ratio of D to H loaded in Pd by the simultaneous electrolysis has been shown to be 0.1. Since the loading process in Pd is absorption-controlled from the result of the separate electrolysis, it is concluded that the flux ratio of ϕ_{D^+}/ϕ_{H^+} is 0.1 in the simultaneous electrolysis. The flux ratio of $\phi_{D^+}/\phi_{H^+} = 0.1$ is very consistent with the well-known ratio of ionization probabilities of D^+ to H^+ estimated from the ionization quotient of H_2O and D_2O [12,13].

5.2. Electrolysis with Zr

It has been also shown that the isotope ratio of D to H loaded in Zr in the separate electrolysis is about 1.5. Since the value of ϕ_{D^+}/ϕ_{H^+} is unity in the separate electrolysis of the present study, this isotope ratio gives that

$$\frac{\left(\sqrt{K^{DD}}/\xi_{ab}^{D}\right)}{\left(\sqrt{K^{HH}}/\xi_{ab}^{H}\right)}$$

is equal to 1.5 using $n_{ad}^{H} = \sqrt{\phi_{H^+}/2K^{HH}}$ and $n_{ad}^{D} = \sqrt{\phi_{D^+}/2K^{DD}}$. This fact indicates that the loading process in Zr is ascribed to competition between absorption and recombination, namely recombination-controlled case.

On the other hand, the isotope ratio of D to H loaded in Zr by the simultaneous electrolysis has been shown to be about 1/3. The isotope ratio can be theoretically estimated from Eqs. (8) and (9), using $\phi_{D^+}/\phi_{H^+} = 0.1$ and

$$\left(\sqrt{K^{DD}/K^{HH}}\right)\left(\xi_{ab}^{H}/\xi_{ab}^{D}\right) = 1.5$$

and assuming $A = 1$, to be about 1/3.

It is seen from these facts that the experimental values of the isotope ratio agrees excellent well with the theoretical ones.

The isotope ratios of D to H loaded in Pd and Zr are concluded to indicate that the loading model proposed in the present study is very much reasonable. These facts therefore are concluded to indicate that the transport and reaction mechanisms of hydrogen isotopes at the metal surface are responsible for the difference between the loading ratios of D to H in Pd and Zr.

6. Conclusion

The loading ratios of protium and deuterium in Zr and Pd have been measured by use of ERDA and SIMS techniques. In the separate electrolysis, the loading ratios of protium and deuterium in Zr are 2.5 and 1.7, and those in Pd are almost the same value, 0.7. On the other hand, in the simultaneous electrolysis, the loading ratio of protium in Pd is 0.7 and that of the deuterium is only 0.07. The isotope ratio is determined by 1/10. whereas, the loading ratio of the protium and deuterium in Zr is almost 1.2 and 0.4, respectively. These results are consistent with the results of the SIMS measurement. The isotope ratio is expressed by 1/3. These results are explained, reasonably by the loading model proposed and the mass balance equations. As a result, the difference between the fluxes of H^+ and D^+ to the Pd cathode mainly bring on the clear isotope effect in Pd. On the other hand, in the Zr case, the amounts of absorbed protium and deuterium are determined both by the absorption conversion effect and the recombination effect.

Acknowledgements

It is our pleasure to thank Professor O. Odawara in Interdisciplinary graduate school of science and engineering, Tokyo Institute of Technology, for his excellent technical assistance in the SIMS measurement.

References

[1] H. Tamura et al., Hydrogen storage alloys, in: Fundamentals and Frontier Technology, NTS Inc., Japan, 1998 (in Japanese).
[2] Y. Fukai, J. Less-Common Met. 101 (1984) 1.
[3] B. Tsuchiya, K. Morita, J. Nucl. Mater. 233–237 (1996) 898.
[4] B. Tsuchiya, K. Morita, J. Nucl. Mater. 233–237 (1996) 1213.
[5] J. Roth, J. Nucl. Mater. 93&94 (1980) 601.
[6] W.R. Wampler, J. Nucl. Mater. 102 (1981) 304.
[7] H.H. Anderson and J.F. Ziegler, Hydrogen Stopping Powers and Ranges in All Elements, vol. 3, Pergamon, Oxford, 1997.
[8] J.F. Ziegler, Helium Stopping Powers and Ranges in All Elements, vol. 4, Pergamon, Oxford, 1997.
[9] S. Nagata et al., Nucl. Instrum. Meth. B 6 (1985) 533.
[10] A. Benninghoven, F.G. Rudenauer, H.W. Werner, Chemical Analysis Series, 86, Wiley, New York, 1987.
[11] A. Lodding, Chemical Analysis Series, 95, Wiley, New York, 1988.
[12] R.E. Mesmer, D.L. Herting, J. Solution Chem. 7 (1978) 901.
[13] D.W. Shoesmith, W. Lee, Can. J. Chem. 54 (1976) 3553.